JOURNAL OF OPTOELECTRONICS AND ADVANCED MATERIALS, Vol. 11, No. 11, November 2009, p. 1788 - 1793

Microcellular carbon from polyacrylonitrile precursors

G. NAN, I. STAMATIN[a*], A. ANDRONIE[a], Ş. IORDACHE[a], C. CRISTESCU[a], A. CUCU[a], A. BACIU, G. A. RIMBU[b]
Petroleum-Gas University of Ploieşti, Physics Department, Bd. Bucureşti 39, Romania
[a]*3Nano-SAE Research Centre, University of Bucharest, PO Box MG-38, Bucharest-Măgurele, Romania*
[b]*INCDIE ICPE-CA, 313 Splaiul Unirii, P. O. Box 149, Bucharest 030138, RO*

Microcellular carbon (CMC) is a distinct material obtained by the polymer matrix pyrolysis containing hard fusible and inert micronized materials by comparison with carbon foam where usual the pyrolized polymers are foamed with different agents. The microcellular carbon is an advanced material due to its properties related to inertness and thermal conductivity where high rate of heat exchange is required and its application to gas separation due to chemical properties from functional groups and controlled pore sizes. This contribution deals with the structural and morphological investigation for CMC resulted from polyacrylonitrile blended with various grain size salts. The pyrolysis and the thermal treatment of the composite has been performed up to 700 ^{0}C.

(Received September 21, 2009; accepted November 12, 2009)

Keyword: Microcellular carbon, Polymer pyrolysis

1. Introduction

Two categories of carbon materials with high porosity are derived from polymer pyrolysis, carbon foams respective microcellular carbon. They are designed for main applications in thermal management, catalyst support and molecular sieves. The carbon foams were developed by Walter Ford, 1960 [1]. The carbon foams were developed as requirements in thermal management of electronics and aircraft parts where high thermal conductivity, low weight and thermal expansion coefficient at high specific strength is required [2]. Usually the carbon foams are originated of the pyrolysis of a thermosetting organic polymer with foaming agent to obtain reticulated vitreous (glassy) carbon foam (RVC). Another route for RVC emerged in the 1990s is based on pitches and coal precursors where mass loss is over 60% and pore dimensions reach few micrometers [3]. Their properties have been extensively studied in the past decades targeting applications such as: thermal protection coating of airspace vehicles [4, 5], bony prostheses [6], heart valves [7-9], and molecular sieves [10], porous electrodes for energy storage and gas filtration [11]. Generally, the pore sizes of RVC fabricated with traditional foaming processes [12-18] are around 200–600 μm in a large uncontrolled distribution. However, RVC with mean pore size smaller than 200 μm can be expected to be applied as biological carbon [19], catalyst supports, filters and foam-reinforced composites [20-22]. The second class, microcellular carbon (CMC) is more or less reticulated carbon resulted from polymer pyrolysis where the pores network is shaped by a high infusible and stable component made of particles/nanoparticles of inert materials which are inserted in the initial polymer matrix. This class respond to the requirements to develop carbon microstructures with a controlled microporous structures (pore diameters in a tight distribution), for application in microultrafiltration, gas storages which could not be reached by foaming agent. Both, CMC and RVC are an interconnected three-dimensional graphitic-like microstructure arranged in a cellular fashion, the only difference consisting of the method to induce the pores network, resulted from the pyrolysis of precursor materials, additives and heat treatment. This contribution deal with designing of CMC resulted from polyacrylonitrile pyrolysis from preshaped tablets with two range in grain size of sodium chloride to show how the size and pore shapes are changing. In addition we proved that the morphology of the carbon is strongly dependent of interface properties polymer-salt particles.

2. Experimental

Materials: Polyacrylonitrile powder (PAN) (Sigma Aldrich) with glass transition T_g = 85^{0}C. Sodium chloride (NaCl) powder technical grade sieved in two ranges: A) 100-300 microns and B) under 60 microns.

Preparation of samples: PAN powder was mixed with 10% wt, salt A respective B and pelletized by pressing under 850 kgf/cm^2 in disc shape 30x0.5 mm.

Thermal treatment

PAN powder was first analyzed by TG and DSC to establish the optimum parameters for pyrolysis and thermal treatment (to evaluate the oxidation stages following by cyclization) at a rate of 10 ^{0}C/ min, air atmosphere. In figure 1 are observed, glass transition at 84.6 ^{0}C and peaks associated with a fast transition from dehydrogenation and cyclization of PAN at 323.9 ^{0}C (DSC curve) assigned to the stages I and III. The temperature of start transformation was indexed on TGA curve at ~312^{0}C. The melting point is not observed due to a slow temperature rate and is consistent with data reported in literature [23]. With the temperature raising the oxidation process and cyclization in normal atmosphere continue at a

slow rate of mass loss until are formed structures of type (IV). Based on these considerations was performed a thermal treatment as follow:

The first stage: temperature was raised slowly up to 400 ^{0}C for 3 hours in normal atmosphere (air). At set point 400^{0}C the samples were kept for 30 minutes to full fill the thermostabilization (dehydrogenation, oxidation and cyclization) with developing of pyridine cycles network.

The second stage: temperature was raised from 400 ^{0}C to 700 ^{0}C (under NaCl melting point) in an hour with inert atmosphere argon at a flow rate of 270-290 sccm/min. At set point 700 ^{0}C the samples are kept 30 minutes. The samples were free cooled to room temperature keeping Ar atmosphere. Finally salt was removed by multiple sonications in water until constant weight is reached.

Characterizations:

Thermal analysis: Mettler Toledo equipment, model TGA/DSC1 Star System with associated software for thermal effect analysis. The microstructure and composition: Scanning Electron Microscopy with EDAX system (SEM, FEI -Quanta 400), Raman spectroscopy (JASCO NRS-3100, laser wavelength λ = 532 nm) and FTIR (spectrometer FT-IR Jasco 6200). For FT-IR analysis CMC samples were pressed in tablets with dried KBr. For SEM and Raman spectroscopy the samples were analysis as resulted from thermal treatment.

3. Results and discussions

The mass loss after thermal treatment is in average 60% wt which is an agreement with TG curve for PAN powder (figure 1). By comparison with the transformation processes which take place with temperature (scheme in figure 1) TG/DTG-DSC curves show oxidation process with water molecules desorbtion respective cyclization of PAN in fused pyridine cycles (IV). The oxidation and cyclization are superimposed processes with exothermic effects reaching maximum temperature of 324 ^{0}C. Water desorbtion as by products takes place between 311 ^{0}C and 340 ^{0}C (DTG curve). With the temperature increasing the oxidative process continue at slow rate on the pyridinic fused cycles (figure 1, IV) until partial degradation with carbonized residuum. When the thermal treatment continues from 400 ^{0}C in inert atmosphere the processes move to route V with releasing HCN. Finally the pyridinic cycles are fusing into an aromatic carbon structure. Their size is dependent of carbonization temperature, respective of number and length of pyridinic cycles which cooperate to generate carbon structures with different level of organization. Thermal analysis of CMC obtained after thermal treatment at 700 ^{0}C is shown in figure 2. CMCs are thermally stable up to 426 ^{0}C where superficial thermoxidative processes on grain size take place. It is assumed that the dangling bonds, nitrogen and other functional groups are involved. The by products desorption is displaced to 580 ^{0}C and finished to 800 ^{0}C where a bulk oxidative process is observed. After this temperature takes place the carbon oxidation.

The microstructure is strongly dependent of NaCl salt grain size. For rough grain size salt type A the microstructure is made of large interconnected pores (cells) resulted from NaCl removal and intergranular mesopores defined by carbon particles. In figure 3.a on SEM images show a microcellular structure in a sponge-like irregular arrangement. The microcellular structure is defined of carbon particles with atypical spheroidal shapes with multiple defects and heterogeneous grain size. The cells size is not in direct relation with salt grain size due to the pressing process where the salt is dimensional reduced by microfragmentation. With small grain size salt (type B) the microstructure is changed. CMC is defined by spheroidal shapes carbon particles. The pores are defined by voids between grains in contact (figure 3.b). The surface of the carbon particles is smooth but with large superficial defects. Due to there is no interaction between salt and PAN respective fused pyridine cycles the carbonization takes place by contraction of these in shapes corresponding to minimum surface energy. The microstructures resulted with fine grain size salt is a new form of carbon materials similar as structure with sintered ceramics in consequence as a carbon ceramic. Topographic analysis on down scale of magnification reveals macropores with rough salt and intergranular pores for fine salt (figures 3.a, b, scale 500 and 100 microns). The carbon materials resulted by the fusion of pyridinic cycles and carbonization at 700^{0}C show spheroidal structures with large defects and fractures respective a randomized intrapores defined by holes developed due to particle contraction (figures 3.a, 4.a, 20 microns). With fine salt the spheroidal particles in random distribution is observed (figure 3.b, 100 microns). In addition on the particle surface are developed large defects made of superficial holes (figures 3.b, 4.b, 20 microns). It can be concluded the salt grain size define a variety of CMC spanning from microcellular to mesoporous structures

The composition investigated by EDAX (fig. 4) shows no dependence of salt grain size and in consequence the mechanisms follow the same route to carbonization. EDAX analysis for composition give an atomic ratio N/C of 0.23-0.25 which is close to that theoretical estimate of 0.33. These results are in agreement with values reported in [26] at similar temperatures. The oxygen concentration is around of 10-11% wt assigned to atomic fraction, O/(C+N)~ 0.07. By comparison the composition by EDAX with thermogravimetry and DSC we conclude that the carbon structures are in early stage of carbonization where the main components have pyridinic structure. Raman spectroscopy (figure 5) show a large band centred on 1345 cm^{-1} assigned to D- band and G- band at 1582 cm^{-1}. The intensity ratio is close to 2 which correspond to large disordered arrangement of the graphenes into carbonized spheroidal particles and in agreement with results reported on glassy carbon [27].

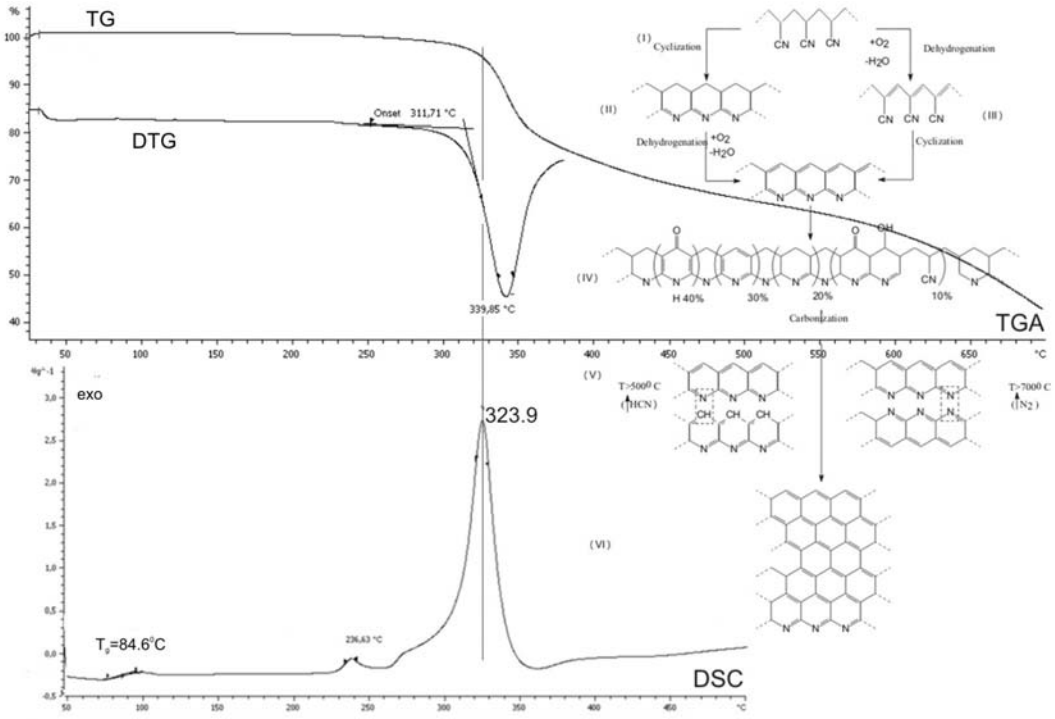

Fig. 1. TG/DTG-DSC curves for PAN powder. TG curve (the temperature of start transformation was indexed at ~312^{0}C). DSC curve (glass transition at 84.6 ^{0}C and peak associated with a fast transition from dehydrogenation and cyclization of PAN at 323.9 ^{0}C). Mechanistic pathways for the thermal degradation of PAN and reactions involved in the stabilization of PAN, after Fitzer et al. [24] and Fitzer [25].

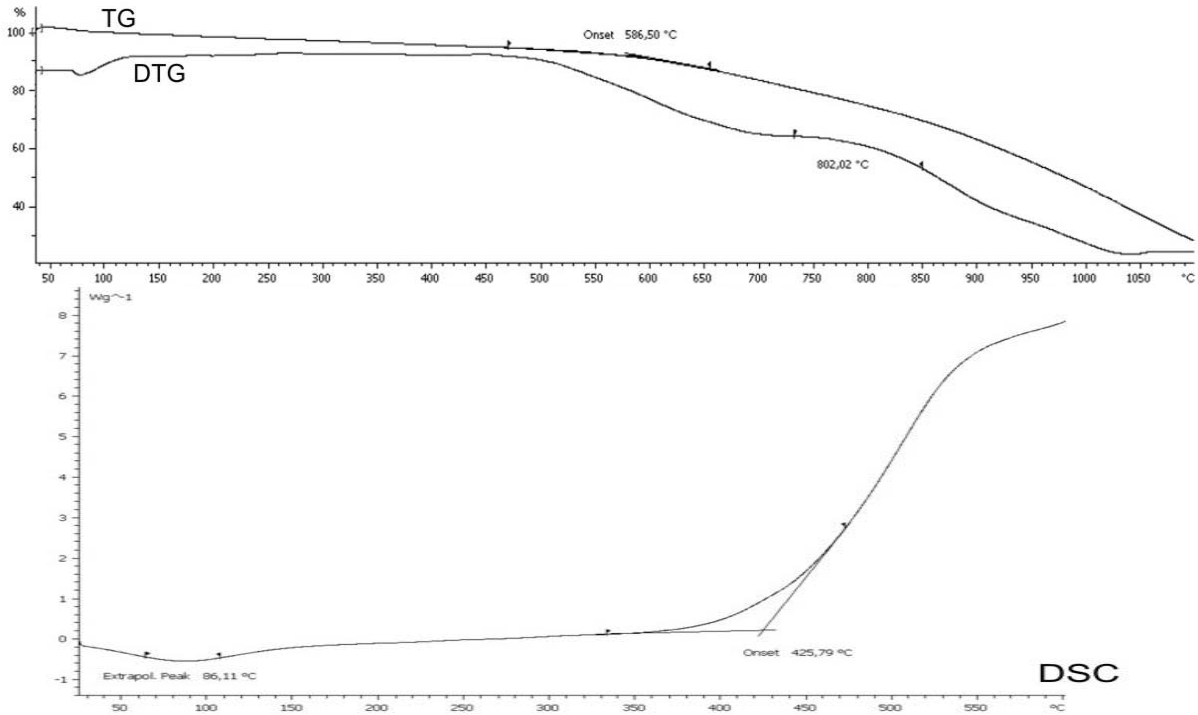

Fig. 2. TG/DTG-DSC curves for CMC. TG curve (desorption is displaced to 580 ^{0}C and finished to 800 ^{0}C where a bulk oxidative process is observed), DSC curve (to 426 ^{0}C superficial thermoxidative processes)

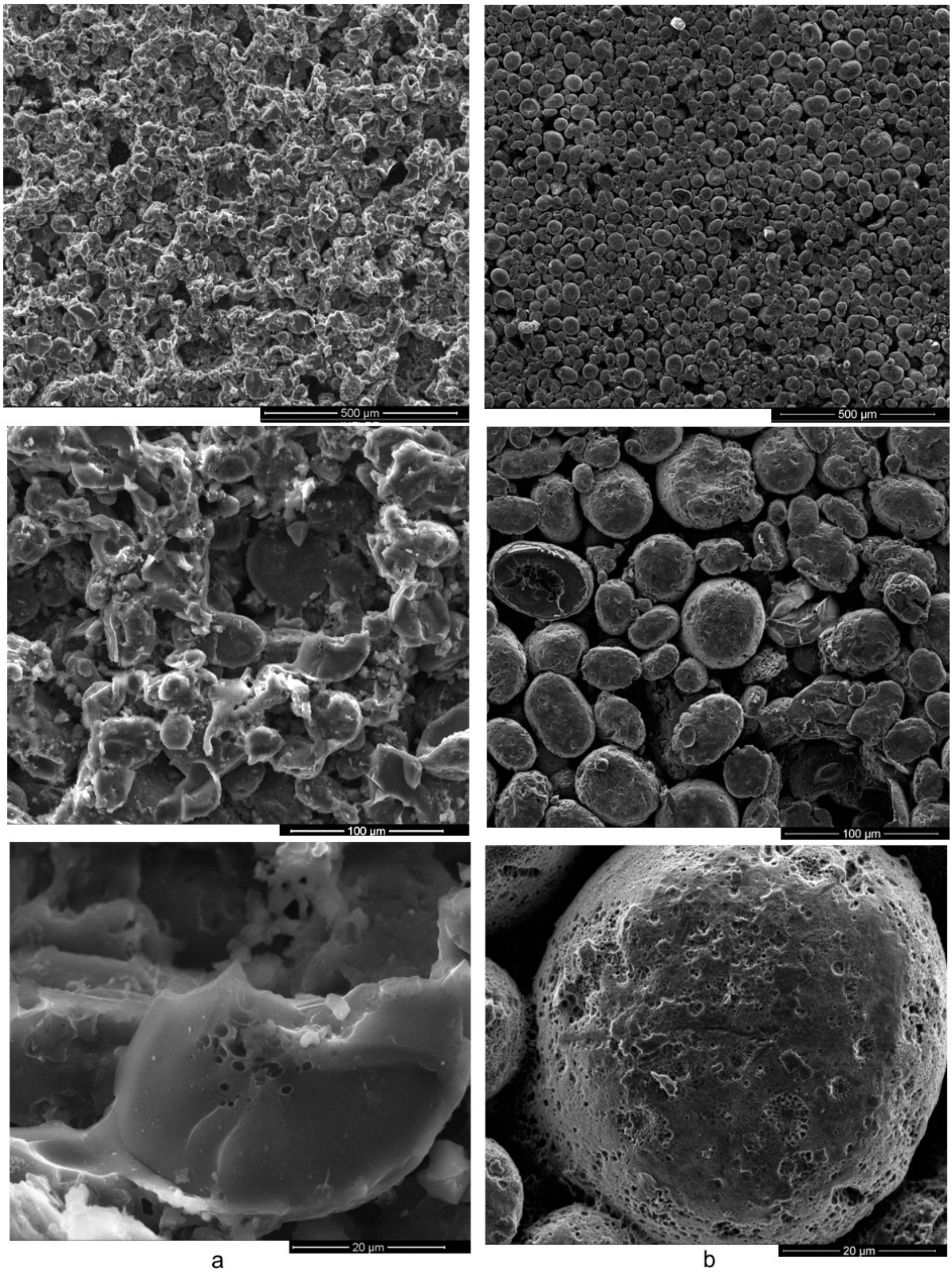

Fig. 3. SEM images for CMC: a) and b) scales 500, 100 and 20 microns

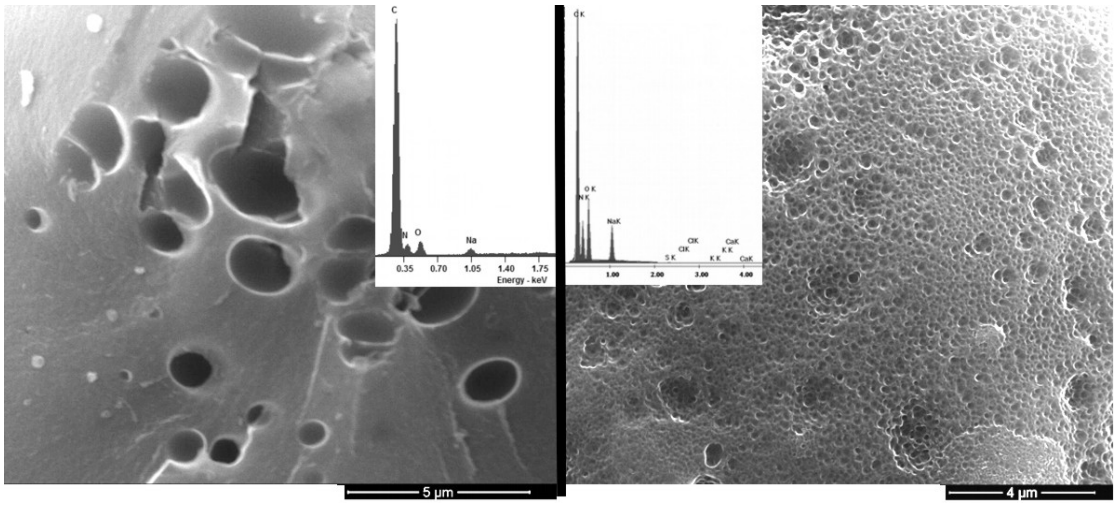

Fig. 4. EDAX analysis for CMC.

Fig. 6 show the FTIR spectrum for CMC. FT-IR spectrum reveals specific features corresponding to fused pyridines cycles agreement. The nitrile groups (C≡N, 2243 cm^{-1}) disappear after heat treatment at 700°C, in association with an increasing in intensity of the band centered on 1104 cm^{-1} assigned to C-N.

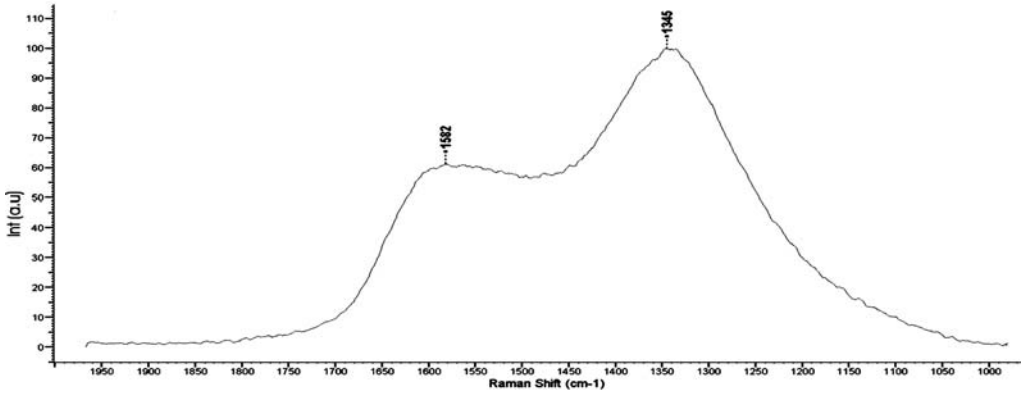

Fig. 5. Raman spectrum for CMC

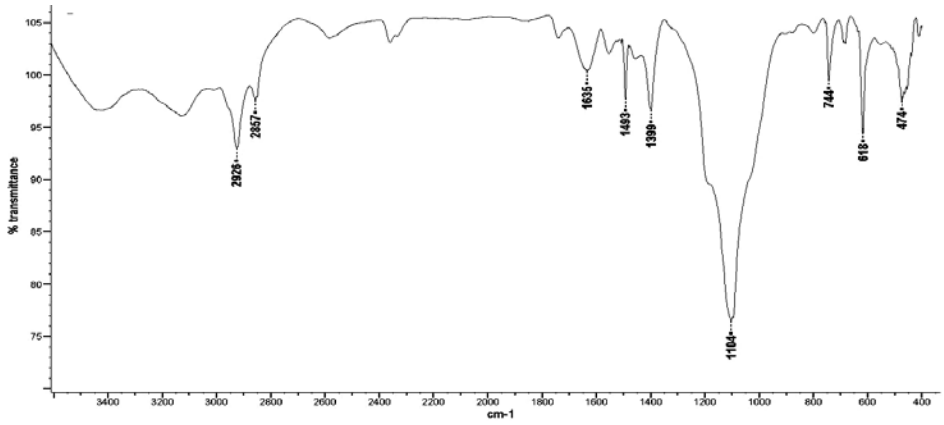

Fig. 6. FT-IR spectrum for CMC obtained at 700°C.

The features for pyridines are frequencies for C-N (1104 cm^{-1}, 1399 cm^{-1}), C=N (1635 cm^{-1}), C=C (1493 cm^{-1}), N-H (3453 cm^{-1}) and C-H stretching (symmetric 2926 $cm^{-1}$and asymmetric 2857 cm^{-1}). Due to the oxidative processes appear supplemental frequencies with weak intensities assigned to O-H stretching at 3117 cm^{-1} and C=O (ketone) at 1743 cm^{-1}.By comparison with Raman spectrum where D band is dominant and FT-IR spectrum it can be concluded the materials is made up of structures (IV) and (V) (figure 1) packed into small spheroidal particles (figure 3)

4 Conclusions

CMCs obtained from PAN pyrolysis in presence of infusible salt exhibit a specific microstructure of spheroidal carbons with pores and shapes which can be tuneable by salts with different grain size. CMC obtained at 700^0C exhibits intermediate structures between fused pyridine cycles and amorphous glassy carbon. The pores shapes are large and not well organized for rough salt grain size respective defined by voids created by intergranular contacts among the spheroidal granules for fine grain size salt.

References

[1] W. Ford, Method of making cellular refractory thermal insulating material, US patent 3121050, (1964).

[2] W. Shih, Development of Carbon-Carbon Composites for Electronic Thermal Management Applications, IDA Workshop, May 3–5, (1994).

[3] J. W. Klett, A. D. McMillan, N. G. Gallego, T. D. Burchell, C. A. Walls, Carbon **42**(8–9), 1849 (2004).

[4] W. G. Bradshaw, P. C. Pinoli, M.J . Mitchell, Recent Developments in glassy carbon fabrication, In: Proceedings of 9th Biennial Conference on Carbon, (1969); Boston: USA, Boston: American Carbon Society, p. 7, (1969).

[5] L. R. Bunnell, Proc. Vitreous carbon matrix carbon-carbon composite by copyrolysis, In: Proceedings of 12th Biennial Conference on Carbon; Pennsylvania, (1975); USA, Pennsilvania: American Carbon Society, p. 333-334, (1975).

[6] R. B. Kaplan, Open cell tantalum structures for cancellous bone implants and cell and tissue receptors, US Patent 5282861, (1994).

[7] M. C. Rezende, Produção de Carbono Vítreo, em Escala de Laboratório, a partir de Resinas Furfurílica e Fenólica, São Paulo, Brazil, (Doctoral Thesis), São Paulo, EPUSP, (1991).

[8] J. C. Bokros, Carbon biomedical devices, Carbon, **15**(6) 353, (1977).

[9] G. M. Jenkins, C. J. Grigson, J. Biomed. Mater, Res. **13**, 371 (1979).

[10] Jr. J. L. Schmitt, P. L. Walker, Carbon, **10**(1), 87 (1972).

[11] B. J. Cooper, D. L. Trimm, Preprint 3rd Conference on Industrial Carbon and Graphite, (1970), London: UK. London: Soc. Chem. Ind., p. 49, (1970).

[12] J. W. Klett, A. D. McMillan, N. G. Gallego, T. D. Burchell, C. A. Walls, Carbon **42**(8–9), 1849 (2004).

[13] T. Beechem, K. Lafdi, A. Elgafy, Carbon **43**(5), 1055 (2005).

[14] M. X. Wang, C. Y. Wang, T. Q. Li, Z. J. Hu, Carbon **46**(1), 84 (2008).

[15] M. X. Liu, L. H. Gan, F. Q. Zhao, X. Z. Fan, H. X. Xu, F. R. Wu et al., Carbon **45**(15), 3055 (2007).

[16] S. Z. Li, Q. G. Guo, Y. Song, Z. J. Liu, J. L. Shi, L. Liu et al., Carbon **45**(14), 2843 (2007).

[17] Y. Chen, B. Z. Chen, X. C. Shi, H. Xu, Y. J. Hu, Y. Yuan et al., Carbon **45**(10), 2132 (2007).

[18] J. Klett, Process for making graphite foam, US Patent 6033506, (2000).

[19] M. Eiroa, A. Vilar, C. Kennes, M.C. Veiga, Bioresource Technology **99**(9), 3507 (2008).

[20] R. V. R. A. Rios, M. M. Escandell, M. M. Sabio, F. R. Reinoso, Carbon **44**(7), 1448 (2006).

[21] M. X. Liu, L.H. Gan, F.Q. Zhao, H.X. Xu, X.Z. Fan C. Tian et al., Carbon **45**(13), 2710 (2007).

[22] X. Xiong, J.H. Li and B.Y. Huang, Carbon **45**(13), 2692 (2007).

[23] M. Lewin, Eli M. Pearce, Handbook of Fiber Chemistry, Second edition, p. 920, (1998).

[24] E. Fitzer, W. Frohs, M. Heine, Carbon **24**, 387 (1986).

[25] E. Fitzer, Acta Polym. **41**, 381 (1990).

[26] C. Jr. Arnold, J.H. Aubert, R.L. Clough, P. B. Rand, A.P. Sylwester, Low density microcellular carbon foams and method of preparation, US Patent 4832881, (1989).

[27] M. I. Nathan, J. E. Smith Jr, K.N. Tu, Journal of Applied Physics, **45**, 2370 (1974).

*Corresponding author: office@3nanosae.org